Evidence of denser $MgSiO_3$ glass above 133 gigapascal (GPa) and implications for remnants of ultradense silicate melt from a deep magma ocean

Motohiko Murakami[a,1] and Jay D. Bass[b]

[a]Department of Earth and Planetary Materials Science, Graduate School of Science, Tohoku University, Sendai 980-8578, Japan; and
[b]Department of Geology, University of Illinois, 1301 West Green Street, Urbana, IL 61801

Edited by David Walker, Columbia University, Palisades, NY, and approved August 31, 2011 (received for review June 16, 2011)

Ultralow velocity zones are the largest seismic anomalies in the mantle, with 10–30% seismic velocity reduction observed in thin layers less than 20–40 km thick, just above the Earth's core-mantle boundary (CMB). The presence of silicate melts, possibly a remnant of a deep magma ocean in the early Earth, have been proposed to explain ultralow velocity zones. It is, however, still an open question as to whether such silicate melts are gravitationally stable at the pressure conditions above the CMB. Fe enrichment is usually invoked to explain why melts would remain at the CMB, but this has not been substantiated experimentally. Here we report in situ high-pressure acoustic velocity measurements that suggest a new transformation to a denser structure of $MgSiO_3$ glass at pressures close to those of the CMB. The result suggests that $MgSiO_3$ melt is likely to become denser than crystalline $MgSiO_3$ above the CMB. The presence of negatively buoyant and gravitationally stable silicate melts at the bottom of the mantle, would provide a mechanism for observed ultralow seismic velocities above the CMB without enrichment of Fe in the melt. An ultradense melt phase and its geochemical inventory would be isolated from overlying convective flow over geologic time.

dynamics | early Earth evolution | high-pressure experiment | sound velocity measurement | pressure-induced polymorphism

The buoyancy relations between silicate melts and crystals in a deep terrestrial magma ocean are the primary constraints on the possible chemical stratification of Earth's interior (1, 2). The nature of silicate melts under high-pressure conditions is therefore critically important for elucidating the formation and differentiation of the Earth through massive primordial melting of the proto-Earth. Extensive melting of the proto-Earth and the formation of a deep magma ocean, induced by massive planetesimal collisions and possibly encompassing an entire planet, facilitated metal-silicate (core-mantle) segregation, with the subsequent fractional crystallization of silicate melt leading to chemical and gravitational equilibrium (3–6). Because of the high compressibility of melts, a density crossover between crystals and coexisting magmas is expected in the course of fractional crystallization in a deep magma ocean, which would enhance chemical differentiation and could result in a stratified structure of the Earth's interior (7, 8). The possible presence of dense, gravitationally stable magmas deep within the Earth at pressures above 100 gigapascals (GPa) has thus been proposed as a consequence of partial melting and a remnant of a deep magma ocean (9, 10), which might explain the observation of anomalously ultralow seismic velocities (ULVZ) above the core-mantle boundary (CMB) (11). However, the behavior of silicate melts under such extreme pressures is poorly understood, and it is still an open question as to whether a density crossover between silicate melt and coexisting mantle phases occurs in the D′′ region above the CMB (approximately 2,900 km depth). Density measurements on silicate melts at relatively low pressures below 15 GPa suggested that gravitationally stable melt compositions in the deep interior are restricted to iron-rich compositions such as basaltic melts (7, 8). The high densities of magnesium-silicate perovskite, (MgFe)O ferropericlase, and Ca-perovskite—the main phases in the lower mantle—make it difficult for melts to be negatively buoyant under lowermost mantle conditions. Although measurements on silicate melts at high pressures are beyond current experimental capabilities, $MgSiO_3$ glass can be used as an analogue for the most abundant component of the silicate melts in a deep magma ocean (12). Experimental investigations of the high-pressure structure of the $MgSiO_3$ glass up to a pressure of 39 GPa strongly suggest that changes in the Si-O and Mg-O coordination number are a critical to the densification mechanism of $MgSiO_3$ glass (13, 14). However, little is known about further densification above approximately 40 GPa due to experimental challenges and the lack of suitable in situ structural probes. In comparison with spectroscopy on crystals, the significant signal weakening and broadening in studying the structure of glasses/melts has so far prevented experiments under extreme high-pressure conditions. Acoustic wave velocity measurements are one of the most promising approaches for detecting structural changes of glasses and melts, inasmuch as the sound velocity directly reflects the density and elasticity, regardless of whether a sample is crystalline or amorphous. Our newly developed in situ high-pressure Brillouin scattering spectroscopic system has recently proven to be highly suitable for measuring acoustic velocities under ultrahigh pressure conditions of approximately 200 GPa (15, 16), corresponding to a depth of approximately 3,500 km in the Earth and thereby permitting the simulation of pressures in a deep magma ocean. Here we report in situ Brillouin scattering results for $MgSiO_3$ glass at pressures up to 203 GPa, revealing a systematic change in the velocity-pressure trajectory above 130 GPa. We infer this to be a unique transition to a denser structure that is likely associated with the onset of a change in coordination number to higher than sixfold.

Results and Discussion

Very sharp Brillouin peaks from the transverse acoustic modes of $MgSiO_3$ glass were obtained over the entire pressure range up to 203 GP, as shown in Fig. 1. We did not observe peaks from longitudinal acoustic waves at pressures higher than 40 GPa. The longitudinal modes were masked by those of the diamond transverse acoustic modes. The full width at half maximum of the transverse acoustic peaks at lower pressure (Fig. 1*A*) and higher pressure (Fig. 1*B*) were identical within the uncertainties [0.44(3) and 0.46(3) GHz, respectively], and no significant peak broaden-

Author contributions: M.M. designed research; M.M. performed research; M.M. and J.D.B. contributed new reagents/analytic tools; M.M. analyzed data; and M.M. and J.D.B. wrote the paper.

The authors declare no conflict of interest.

This article is a PNAS Direct Submission.

Freely available online through the PNAS open access option.

[1]To whom correspondence should be addressed. E-mail: motohiko@m.tohoku.ac.jp.

This article contains supporting information online at www.pnas.org/lookup/suppl/doi:10.1073/pnas.1109748108/-/DCSupplemental.

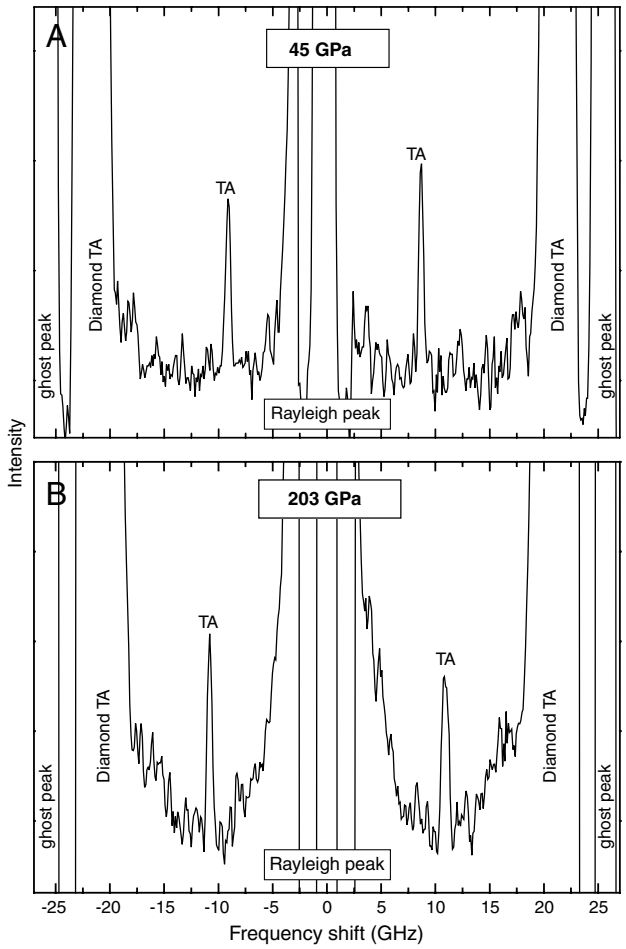

Fig. 1. High-pressure Brillouin spectra at 45 GPa (*A*) and 203 GPa (*B*). TA: transverse acoustic mode of $MgSiO_3$ glass.

ing was observed with pressure (Fig. S1 and Table S1). This indicates that the hydrostaticity in the sample chamber did not change drastically with increasing pressure. Such high quality Brillouin scattering signals under extreme pressure conditions resulted in velocity uncertainties of 0.6% on average throughout the pressure range we explored (Table S1). Fig. 2 shows the results for the transverse acoustic wave velocities for $MgSiO_3$ glass as a function of pressure together with those of SiO_2 glass that we recently reported (16).

All data were fit by polynomial functions to evaluate the change in trend of the transverse acoustic wave velocity of $MgSiO_3$ glass as a function of pressure, which gives a remarkably good fit with an adjusted *R*-square of 0.9986 as shown in Fig. 2. The pressure at which the change in trend of the velocity profile occurs was then determined by evaluating the second derivative of the fitted function with respect to the pressure and determining the point at which d^2V_T/dP^2 is a maximum. This point was found to be at 133 GPa. The transverse acoustic wave velocity of $MgSiO_3$ glass increased continuously from 12 to 133 GPa in a convex-upward trend. The pressure derivatives of transverse acoustic velocity (dV_T/dP) from 12 GPa to 133 GPa decrease gradually by one order of magnitude, from 58.5 to 7.4 (m/sec)/GPa. By contrast, we found a significantly steeper velocity trajectory upon subsequent pressure increase from 133 to 203 GPa. This velocity profile is fit well by a logarithmic function with dV_T/dP of 10.2 (m/sec)/GPa at 133 GPa, showing that the velocity gradient increases by approximately 43% compared to the lower pressure trend below 133 GPa (5.3 (m/sec)/GPa).

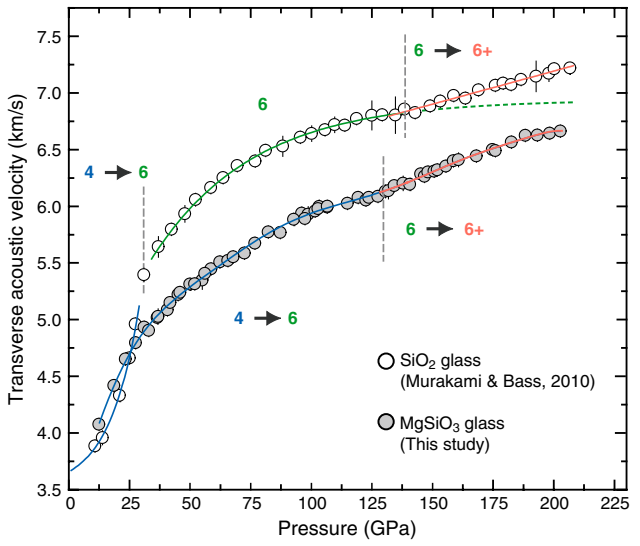

Fig. 2. Transverse acoustic wave velocities of $MgSiO_3$ glass (gray circles) as a function of pressure up to 203 GPa. The white circles indicate the results on SiO_2 glass by Murakami and Bass (16). The velocity trajectories for the distinct pressure regimes are shown as blue, green, and orange lines with increasing pressure. Numbers indicate the potential Si-O coordination number within each pressure regime. Approximate pressure boundary for each Si-O coordinated structure are shown as the vertical dot lines. Error bars are $\pm 1\sigma$ from mean.

In comparison with our recent high-pressure acoustic velocity results on SiO_2 glass (16), we found a remarkably consistent trend with an anomalous velocity gradient increase above 130 GPa (Fig. 2). Our results for SiO_2 glass along with those of previous studies (17–24) indicate that the velocity-pressure trends in SiO_2 glass can be interpreted as a gradual transition from four- to sixfold coordination of Si below 40 GPa, predominantly sixfold coordination from 40 to 140 GPa, and a transition from sixfold to a higher coordination state above 140 GPa (16) (Fig. 2). This notable similarity in the velocity-pressure curves for $MgSiO_3$ and SiO_2 glasses above 130 GPa is a strong indicator that the structural transformation of $MgSiO_3$ glass corresponds to a change in the Si-O coordination number from sixfold to a higher coordination state. The absence of a sharp exponential velocity increase at low pressures, as observed in SiO_2 glass, suggests that the gradual coordination change from four- to sixfold occur over a wider pressure range for $MgSiO_3$ glass (25). Given that the velocity profile of $MgSiO_3$ glass from 40 to 140 GPa always exhibits a steeper trend than that of SiO_2 glass, which is dominated by sixfold coordination (Fig. 2), it is reasonable to expect that the gradual change in Si-O coordination number from four- to sixfold in $MgSiO_3$ glass is continuous over a broad pressure range up to approximately 130 GPa. This is possibly due to the presence of network-modifying Mg^{2+} cations acting to impede the Si-O coordination change from $4 \rightarrow 6$, at least at lower pressures (13, 14). Such a gradual coordination change over a broad pressure range is consistent with recent computational simulations on $MgSiO_3$ melt using first-principles molecular dynamics (25).

Although further experimentation on the effect of temperature and chemistry is needed to obtain insight on the behavior of more realistic magma ocean compositions, the identification of a unique densification mechanism for $MgSiO_3$ glass above 130 GPa, closely matching the pressure at the CMB region (approximately 135 GPa), could have a major affect on the density contrast between melts and coexisting solids phases in a deep terrestrial magma ocean. Previous experiments on amorphous $MgSiO_3$ at pressures below 10 GPa indicate that higher temperature should promote relaxation of the glass, thus making the structural transition to an ultradensified melt at somewhat lower

GEOPHYSICS

pressure (13) and above the CMB. A recent computational study examined the pressure-density relationship between of $MgSiO_3$ melt with predominately six-coordinated Si, and $MgSiO_3$ perovskite, the principal phase in the lower mantle. These simulations show that the densities of melt and $MgSiO_3$ perovskite converge as the pressure of the CMB is approached, but that the amorphous phase remains positively buoyant (25). The present finding of a unique denser structure of $MgSiO_3$ glass, possibly associated with a Si-O coordination number change to higher than six, is highly suggestive of a density crossover between $MgSiO_3$ melt and coexisting mantle minerals in the deep terrestrial magma ocean that is likely to be achieved near the CMB region. Combining the previous analysis of shock wave Hugoniot results for $MgSiO_3$ (12), $MgSiO_3$ melt that is a few percent denser than crystalline $MgSiO_3$ can be inferred under CMB conditions. Virtually all previous efforts to explain the presence of melt in D″ have invoked a strong partitioning of Fe and possibly Ca into the melt phase, but there is no experimental or theoretical justification for such partitioning at CMB pressure-temperature conditions. Other studies have suggested Fe enrichment of the melt via interaction of with the molten Fe alloy of the outer core. However, experiments have shown that oxides of the lowermost mantle would in fact be depleted in Fe through interaction with molten Fe-rich alloys (26, 27). The ultrahigh density melt state implied by the present study is attained through changes in the atomic structure of the amorphous phase, without the addition of heavy elements such as Fe and Ca to the melt, thereby strengthening models with dense melt at the bottom of Earth's mantle (8–10). With this buoyancy relationship, one can infer possible dynamical behavior of the dense melt in the course of crystallization of a magma ocean in the early Earth, although further investigations are required for more quantitative discussions. Ultradense melts, with whatever inventory of incompatible elements they might concentrate, may be dynamically (and chemically) isolated from convection in overlying solids and melts over geologic time. Partially molten regions may currently persist in the narrow pressure gap between the top of the outer core and the neutral buoyancy line for melt, providing a possible explanation for the distinctively thin structure of ULVZs, which are typically less than 40 km (11).

Because extensive melting of the protoplanets is believed to be almost inevitable during the formation of the terrestrial planets (3–6) it is perhaps likely that gravitationally stable dense magmas in a deep magma ocean are a fairly common phenomenon for the larger terrestrial planets. The presence of such ultradense magma should significantly enhance chemical differentiation, especially in deeper parts of the planets, and would therefore have important implications for the chemical evolution of not only the Earth but also giant extrasolar terrestrial planets, such as recently discovered super-Earth (28).

Methods

The $MgSiO_3$ glass was prepared from the synthetic stoichiometric $MgSiO_3$ gel that has been used for the previous high-pressure experiments on the stability of the $MgSiO_3$ postperovskite phase (29). The gel powder was placed in a platinum crucible, melted in air in a furnace at 1650 °C and quenched by immersing the base of the crucible in water. The composition and homogeneity of the final glass was confirmed by electron probe microanalysis and polarized microscope observation.

In situ high-pressure Brillouin scattering measurements of acoustic wave velocities were performed at room temperature with a symmetric diamond anvil cell, an argon laser ($\lambda = 514.5$ nm) as a light source, and Sandercock-type six-pass tandem Fabry–Perot interferometer to analyze the scattered light. The incident laser beam was focused to a spot size of approximately 20 μm. In all measurements, we used a symmetric scattering geometry with a 50° external scattering angle. A prepressed plate of $MgSiO_3$ glass powder was loaded into a 50 μm hole drilled in the rhenium gasket, without a pressure-transmitting medium. The sample was compressed with 150 μm culet beveled diamond anvils. Pressure was determined using the Raman T_{2g} mode of the diamond anvil (30) by measuring several points around the central area of the sample where the probe laser for Brillouin scattering measurements was irradiated. Representative Raman spectra and their differential spectra $dI/d\nu$ from the different points are shown in Fig. S1. The high-frequency edge of the Raman band was defined as a minimum of the $dI/d\nu$, which is determined by curve fitting using a Gaussian function. As shown in Fig. S1 and Table S1, we obtained very sharp peaks for the $dI/d\nu$ function at each pressure point, even at Mbar pressures, yielding measured pressures that were typically consistent within 1 GPa. Brillouin spectra were collected on the compressed $MgSiO_3$ glass at 59 pressures in two separate runs from 12 to 203 GPa, in pressure increments of 2–6 GPa. The collecting time for a single Brillouin measurement was from 30 min to 12 h. At each pressure, the raw Brillouin spectra of Stokes and anti-Stokes peaks were fitted with a Gaussian function to determine peak locations. Additional experimental details are provided elsewhere (15).

ACKNOWLEDGMENTS. We thank Kohei Hatano for his valuable comments on data analysis, and Ed Stolper and anonymous reviewers for constructive suggestions. This study was supported by the Grant-in-Aid for Challenging Exploratory Research (21654075) by the Ministry of Education, Culture, Sports, Science and Technology, Japan (M.M.), and by the US National Science Foundation through Grants EAR-0738871 and the Consortium for Materials Properties Research in Earth Sciences (COMPRES) EAR 10-43050 (J.D.B.).

1. Stolper EM, Walker D, Harger BH, Hays JF (1981) Melt segregation from partially molten source regions: the importance of melt density and source region size. *J Geophys Res* 86:6261–6271.
2. Ohtani E (1985) The primordial terrestrial magma ocean and its implication for stratification of the mantle. *Phys Earth Planet In* 38:70–80.
3. Stevenson DJ (1990) *Origin of the Earth*, eds HE Newsom and JH Jones (Oxford University Press, Oxford), pp 231–249.
4. Cameron AG, Benz WB (1991) The origin of the moon and the single impact. *Icarus* 92:204–216.
5. Tonks WB, Melosh HJ (1993) Magma ocean formation due to giant impact. *J Geophys Res* 98:5319–5333.
6. Canup RM (2004) Dynamics of lunar formation. *Annu Rev Astron Astr* 42:441–475.
7. Agee CB, Walker D (1989) Static compression and olivine flotation in ultrabasic silicate liquid. *J Geophys Res* 98:3437–3449.
8. Ohtani E, Maeda M (2001) Density of basaltic melt at high presure and stability of the melt at the base of thelower mantle. *Earth Planet Sc Lett* 193:69–75.
9. Labrosse S, Hernlund JW, Coltice NA (2007) Crystallizing dense magma ocean at the base of the earth's mantle. *Nature* 450:866–869.
10. Williams Q, Garnero EJ (1996) Seismic evidence for partial melting at the base of earth's mantle. *Science* 273:1528–1530.
11. Garnero EJ, Revenaugh J, Williams Q, Lay T, Kellogg LH (1998) *The Core-Mantle Boundary Region*, eds M Gurnis, ME Wysession, E Knittle, and BA Buffett (American Geophysical Union, Washington, DC).
12. Akins JA, Luo S-N, Asimow PD, Ahrens TJ (2004) Shock-induced melting of $MgSiO_3$ perovskite and implications for melts in earth's lowermost mantle. *Geophys Res Lett* 31:L14612.
13. Gaudio SJ, Sen S, Lesher CE (2008) Pressure-induced structural changes and densification of vitreous $MgSiO_3$. *Geochim Cosmochim Acta* 72:1222–1230.
14. Lee SK, et al. (2008) X-ray raman scattering study of $MgSiO_3$ glass at high pressure: implication for triclustered $MgSiO_3$ melt in earth's mantle. *Proc Natl Acad Sci USA* 105:7925–7929.
15. Murakami M, et al. (2007) Sound velocity of $MgSiO_3$ post-perovskite phase: a constraints on the D″ discontinuity. *Earth Planet Sc Lett* 259:18–23.
16. Murakami M, Bass JD (2010) Spectroscopic evidence for ultrahigh-pressure polymorphism in SiO_2 glass. *Phys Rev Lett* 104:025504.
17. Hemley RJ, Mao H, Bell PM, Mysen B (1986) Raman spectroscopy of SiO_2 glass at high-pressure. *Phys Rev Lett* 57:747–750.
18. Williams Q, Jeanloz R (1988) Soectroscopic evidence for pressure-induced coordination changes in slicate-glass and melts. *Science* 239:902–904.
19. Meade C, Hemley RJ, Maeda M (1992) High-pressure X-ray diffraction of SiO_2 glass. *Phys Rev Lett* 69:1387–1390.
20. Zha C-S, Hemley RJ, Mao H, Duffy TS, Meade C (1994) Acoustic velocities and refractive index of SiO_2 glass to 57.5 GPa by Brillouin scattering. *Phys Rev B* 50:13105–13112.
21. El'kin F, Brazhkin V, Khvostantsev L, Tsiok O, Lyapin A (2002) In situ study of the mechanism of formation of pressure-densified SiO_2 glasses. *JETP Lett+* 75:342–347.
22. Loerting T, Brazhkin V, Morishita T (2009) Multiple amorphous-amorphous transitions. *Adv Chem Phys* 143:29–82.
23. Lin J-F, et al. (2007) Electronic bonding transition in compressed SiO_2 glass. *Phys Rev B* 75:012201.
24. Sato T, Funamori N (2008) Sixfold-coordinated amorphous polymorph of SiO_2 under high pressure. *Phys Rev Lett* 101:255502.
25. Stixrude L, Karki BB (2005) Structure and freezing of $MgSiO_3$ liquid in earth's lower mentle. *Science* 310:297–299.
26. Ozawa H, et al. (2008) Chemical equilibrium between ferropericlase and molten iron to 134 GPa and implications for iron content at the bottom of the mantle. *Geophys Res Lett* 35:L05308.

27. Ozawa H, et al. (2009) Experimental study of reaction between perovskite and molten iron to 146 GPa and implications for chemically distinct buoyant layer at the top of the core. *Phys Chem Miner* 36:355–363.
28. Rivera EJ, et al. (2005) A ~7.5 earth-mass planet orbiting the nearby star, GJ876. *Astrophys J* 634:625–640.
29. Murakami M, Hirose K, Kawamura K, Sata N, Ohishi Y (2004) Post-perovskite phase transition in $MgSiO_3$. *Science* 304:855–858.
30. Akahama Y, Kawamura H (2004) High-pressure Raman spectroscopy of diamond anvils to 250 GPa. *J Appl Phys* 96:3748–3751.